Eur. Phys. J. Appl. Phys. **88**, 20902 (2019)

https://doi.org/10.1051/epjap/2019190048

THE EUROPEAN PHYSICAL JOURNAL APPLIED PHYSICS

Regular Article

Thermal performance comparison of different sun tracking configurations★

O. Achkari* and A. El Fadar

Laboratory of Innovating Technologies, National School of Applied Sciences, Tangier, Abdelmalek Essaadi University, Morocco

Received: 27 February 2019 / Received in final form: 13 September 2019 / Accepted: 19 December 2019

Abstract. Parabolic trough collector (PTC) is one of the most widespread solar concentration technologies and represents the biggest share of the CSP market; it is currently used in various applications, such as electricity generation, heat production for industrial processes, water desalination in arid regions and industrial cooling. The current paper provides a synopsis of the commonly used sun trackers and investigates the impact of various sun tracking modes on thermal performance of a parabolic trough collector. Two sun-tracking configurations, full automatic and semi-automatic, and a stationary one have numerically been investigated. The simulation results have shown that, under the system conditions (design, operating and weather), the PTC's performance depends strongly on the kind of sun tracking technique and on how this technique is exploited. Furthermore, the current study has proven that there are some optimal semi-automatic configurations that are more efficient than one-axis sun tracking systems. The comparison of the mathematical model used in this paper with the thermal profile of some experimental data available in the literature has shown a good agreement with a remarkably low relative error (2.93%).

1 Introduction

Solar energy market is witnessing unprecedented developments and takes an increasingly important role in the global energy policies. Morocco is no exception to this trend and has the advantage of having a particularly rich potential, with more than 3000 hr/year of sunshine and an irradiation of 5.3 kWh/m^2/day [1], to meet a part of its future energy demand and to reach ambitious climate protection goals. Concentrated solar power (CSP) is among the most mature solar technologies in the energy market [2]; it is one of the widely recognized classes of technologies for converting solar energy into thermal or electric energy.

The improvement of thermal performance and competitiveness of CSP against the conventional fuel-based systems is guaranteed by the use of sun trackers that ensure the continuity of energy production by keeping the aperture area of solar collectors in an optimum position, perpendicular to the sun rays during the daytime. The classification of these devices depends on many different parameters. Based on their operating processes, one can categorize them into two main groups: passive and active trackers [2].

Passive solar trackers track the sun without any mechanical drives; they are based on thermal expansion of a matter or on shape memory alloys, and are usually composed of couple of actuators working against each other which are balanced by equal illumination. By differential illumination of actuators, unbalanced forces are used for orientation of the apparatus in such direction where equal illumination of actuators and balance of forces is restored [2]. Several studies and tests have been conducted to show that passive trackers are competitive to electrically based systems. For instance, Clifford et al. [3] presented a novel passive solar tracker modeled with computer. Their tracker incorporates two bimetallic strips made of aluminum and steel, positioned on a wooden frame, symmetrically on either side of a central horizontal axis. The bimetallic strips are shaded so that the strip further from the sun absorbs solar radiation while the other strip remains shaded. The computer model and experimental data showed results similar to each other. The designed solar tracker had the potential to increase solar system efficiency by up to 23%.

Active sun trackers use sensors and/or programmable controllers as well as the electrical motors for their operation [4]. They are usually categorized as (i) microprocessor and electro-optical sensor based sun trackers (closed loop) and (ii) computer controlled date and time based trackers (open loop). All the electro-optical trackers use pairs of photo sensors which are electrically balanced by receiving equal amount of light and in computer controlled date and time based, a logical unit executes date and time algorithms to determine the sun position and create signals for the motors. Active sun trackers can be either single axis tracking or dual axis tracking. The most commonly used configurations in two axes tracking are azimuth-elevation and tilt-roll (polar), which provide higher accuracy and are well known to

★ Contribution to the Topical Issue Materials for energy harvesting, conversion, storage and environmental engineering (Icome 2018)

* e-mails: oussama.achkari@gmail.com

improve overall captured solar energy by 30–50% compared to a fixed tilt device [5–7]. In the same vein, Maatallah et al. [8] reported that double axes sun trackers have always generated better output power when compared to single axis sun tracker and fixed CSP systems. Many other authors have studied active sun tracking systems to analyze and enhance their impact on the thermal efficiency of CSP systems. For example, Khalifa and Al-Mutawalli [9] performed an experimental study to investigate the effect of using two axes sun tracking system on the thermal performance of compound parabolic concentrator (CPC). The tracking of CPC showed a better performance with an increase in the collected energy of up to 75% compared with an identical fixed collector.

Consistent with the above findings, Barakat et al. [10] designed a two axes closed loop sun tracking system; they found that the energy available to the two axes tracker is higher by 20% when compared with stationary systems. Abdallah and Nijmeh [11] designed and constructed an electromechanical open loop two axes sun tracking system. The results indicate that the measured collected solar energy on the moving surface was significantly larger than that collected on a fixed one by 41.34%. Sun et al. [12] proposed a new optimized tracking strategy for a small-scale double-axes parabolic trough collector that maximizes the amount of the annual received solar radiation by maintaining the PTC at the half-day optimal azimuth angles in the morning and afternoon, shifting at solar noon. The results have shown that this new tracking strategy is efficient in autumn and winter seasons in regions with low and middle latitude.

Always in the perspective of comparative studies between full tracking installation and fixed one, Salsabila et al. [13] have studied the effectiveness of utilizing time and date-based sun positioning solar collector system in tropical climate in Northern Peninsular Malaysia. The system has two axes tracking controlled by a programmable logic controller (PLC). The field test has been done during a sunny and clear day, cloudy day, and heavy overcast and rainy day in which the results showed that the improvement in the generated power was about 58%, 49% and 48%, respectively, as compared with a zenith-facing non-tracking system. Wang et al. [14] studied the solar incident angles and the optical performance of a tracking compound parabolic concentrating solar collector with concentration ratio of 2.3, which combines the CPC, heat pipe evacuated tubular receiver and crank rod transmission mechanism. The simulation results have shown that the average optical efficiency was improved by 60% compared to the fixed mode.

Finally, Qua et al. [15] presented a different sun trucking approach by manufacturing a north-south axis PTC prototype of 300 kWh. Beside the east-west tracking system, this prototype has a rotatable axis which is located at the central disk of the rotatable steel-support frame on the ground; hence, it is capable of rotating 14° from north to east or from north to west. The experimental results pointed out that the measured daily average solar collector efficiency achieves about 38.5% in autumn, with about 7.2% higher than that of conventional north-south axis tracking.

Based on the existing literature, numerous previous works have been devoted to different sun tracking technologies and their characteristics; however they are focused only on comparative studies either between various solar tracking technologies or between stationary collectors and automatic ones following constantly the sun. Unlike the previous works, the key objective of the current paper is to introduce a semi-automatic sun tracking method as an alternative approach that could be energetically more efficient than both stationary and automatic methods, under certain conditions, as the simulation results of this study will put in evidence.

2 System description

In this work, the thermal energy production has been chosen as output energy which will serve as the basis for comparison of different solar tracking configurations. The system used for this purpose is schematized in Figure 1. It is mainly composed of a cylindrical parabolic reflecting surface (concentrator), a receiver tube where the heat transfer fluid circulates and a tracking mechanism. The concentrator is composed of a bunch of reflective surfaces that collect and concentrate incident direct solar radiations onto the focal line. The receiver tube is a coated absorber tube which is covered by glass and placed at the focal line of the parabolic trough mirror. The internal space between the glass and absorber metal is kept under vacuum to reduce convective heat losses. The tracking mechanism is an electronic device that maintains the reflector in the optimal direction by reducing the incidence angle. Its operating principle is mainly based on the calculation of the sun's apparent position using microprocessors.

Hot water storage tank is a thermally insulated recipient where thermal energy produced by solar thermal collectors is stored as sensible heat; it contains a built-in heat-exchanger to heat up cold water. Hot water stored could be then used according to the needs. The design and operating parameters used in simulations are listed in Table 1.

3 Mathematical formalism

3.1 Sun position

The estimation of the instantaneous sun's position was calculated by the most accurate algorithm proposed by Jean MEEUS [16], which gives results with an uncertainty of $\pm 0.0003°$ valid between the years -2000 and 6000. The mathematical equations that describe this algorithm could be found in references [16,17].

3.2 Thermal performance assessment

The instantaneous thermal efficiency of a parabolic trough collector is defined as the ratio between the useful thermal power produced by PTC ($Q_{u,th}$) and the beam solar irradiance (I_b) received by the aperture area collector (A_{ap}).

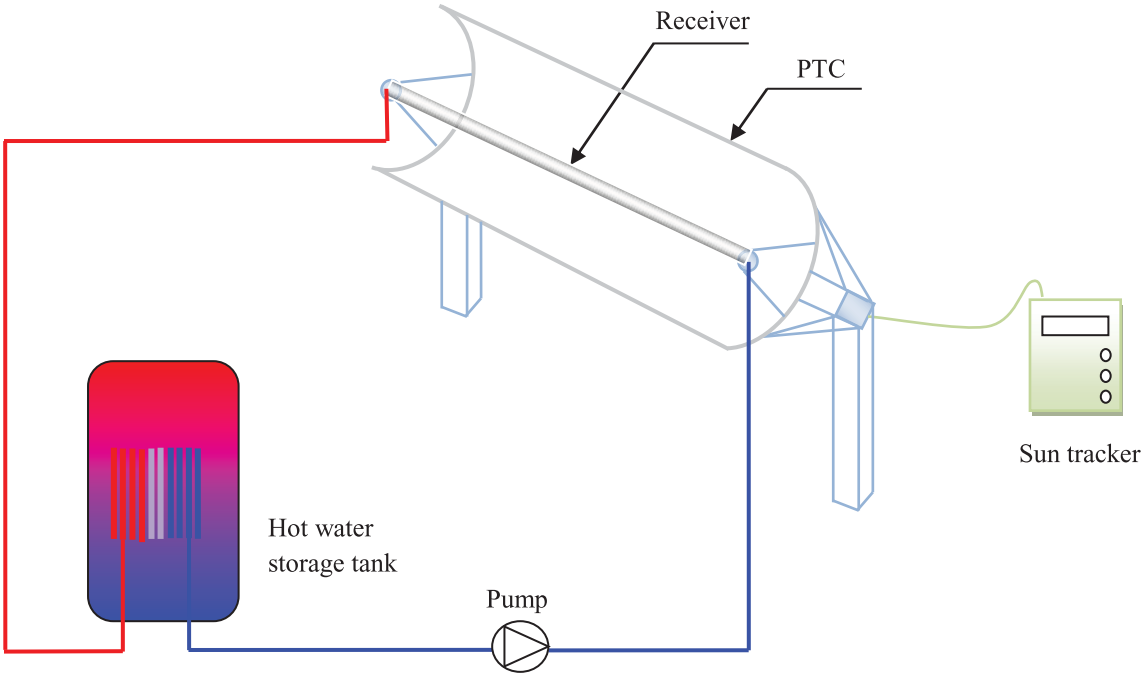

Fig. 1. Scheme of the thermal energy producing system driven by PTC.

Table 1. Main input data used in the simulation.

Parameter	Value	Unit
Collector components		
Collector length	3	m
Aperture width	1.1	m
Inner absorber diameter	0.015	m
Outer absorber diameter	0.019	m
Mirror absorptance	0.87	–
Mirror reflectivity	0.9	–
Receiver conductivity	384	W/m. K
Overall heat loss coefficient	8	$W/m^2.K$
Heat removal factor of collector	0.9	–
Hot water storage tank		
Diameter of the storage tank	0.39	m
Height of the storage tank	0.417	m
Specific heat capacity of water	4.18	kJ/ kg. K
Specific heat capacity of the metal	0.46	kJ/ kg. K
Stored water mass	40	kg
Tank mass	9	kg
Operating conditions		
Fluid flow rate	36	kg/h

It can be calculated by the following equation [18]:

$$\eta_{th} = \frac{Q_{u,th}}{I_b \times A_{ap}}. \quad (1)$$

To evaluate $I_{b,}$ we first calculate the incidence angle θ between the direct sun ray and the normal on the aperture area; it depends on the sun zenith angle θz, the collector tilt angle w, the geocentric sun azimuth angle Γ and the collector azimuth angle γ. It is given by the following relation [18]:

$$\theta = \arccos(\cos\theta_z \times \cos w + \sin w \times \sin\theta_z \times \cos(\Gamma - \gamma)). \quad (2)$$

Then we calculate the direct normal solar irradiance I_{bn} using the following equation [18]:

$$I_{bn} = A_1 \times \exp\left(-\frac{P_L}{P_0} \times \frac{B}{\sin\theta_e}\right) \quad (3)$$

with

$$\frac{-P_L}{P_0} = \exp(0.0001184 \times H_{alt}) \quad (4)$$

$$B = 0.175 \times (1 - 0.2 \times \cos(0.93 \times ND) - 0.0045 \times (1 - \cos(1.86 \times ND)) \quad (5)$$

and

$$A_1 = 1185 \times \left(1 + 0.066 \times \cos\left(360 \times \frac{ND}{370}\right)\right). \quad (6)$$

Finally, I_b can be estimated by [18]:

$$I_b = I_{bn} \times \cos\theta. \quad (7)$$

On the other hand, the useful thermal power depends on the absorbed solar radiation H_{ab}, the fluid temperature in storage tank and the two coefficients of thermal losses F_R and U_l It is estimated by [19]:

$$Q_{u,th} = A_{ap} \times F_R \left(H_{ab} - \frac{A_{r,ext}}{A_{ap}} \times U_l \times (T_{in} - T_{amb}) \right) \tag{8}$$

and

$$Q_{u,th} = m_f \times C_p (T_{out} - T_{in}) \tag{9}$$

with

$$U_l = h_w + h_{r,r-a} \tag{10}$$

and

$$F_R = \frac{m_f C_P}{A_{r,int} \times U_l} \times \left(1 - \exp\left(\frac{-A_{r,int} \times U_l \times F^{-}}{m_f C_p} \right) \right). \tag{11}$$

For a receiver with an inlet diameter $D_{r,int}$, an outlet diameter $D_{r,ext}$ and a convective heat transfer coefficient with the fluid hc,i, the efficiency factor of collector F^{-} is estimated by the following formula [20]:

$$F^{-} = \frac{\frac{1}{U_l}}{\frac{1}{U_l} + \frac{D_{r,ext}}{h_{c,i} \times D_{r,int}} + \frac{D_{r,ext} \times \ln\left(\frac{D_{r,ext}}{D_{r,int}}\right)}{2 \times K_r}}. \tag{12}$$

The absorbed solar radiation H_{ab} is estimated in function of the beam solar irradiance (I_b), the absorptance (α) and the reflectivity of the reflector (ρ), as follows [18]:

$$H_{ab} = I_b \times \alpha \times \rho. \tag{13}$$

As for the inlet temperature of the receiver (T_{in}), it will be calculated by discretizing the following differential formula [21]:

$$\begin{aligned} &\left(M_{st} \times C_p + M_{met} \times C_{pmet}\right) \times \frac{dT_{st}}{dt} \\ &= m_f \times C_p \times (T_{out} - T_{in}) + U_l \times A_{st} \\ &\quad \times (T_{amb} - T_{st}). \end{aligned} \tag{14}$$

4 Numerical procedure

As developed above, the theoretical model consists of two main parts: solar radiation model and thermal model. All parameters of this model are calculated at each time step of ten minutes according to the numerical scheme detailed as follows:

Regarding the solar radiation model, inputs are latitude, longitude, month, day, and local time. All the sun-earth equations are implemented in a computer program written in MATLAB to calculate the sun elevation angle and sun azimuth angle, the angle of incidence and then the direct solar radiation. In this model, an additional function is used to calculate the rotation's step of the sun tracker to align the normal vector of the aperture area with the same plane of the direct sun rays. It represents the difference between the zenith angle of the sun at two consecutive instants t and $t+\Delta t$, where Δt represents the time step. Since the sun tracker is equipped with a stepper motor, this function has an optimization algorithm so that the result is always an integer; indeed if the decimal digit of the new rotation's step is lower than 0.2° or higher than 0.7°, the latter is rounded down or up respectively to eliminate the fraction, otherwise the integer part of the new rotation's step is incremented by 0.5°. Moreover, this function determines also the direction of the motor's rotation according to the sign of the rotation's step.

On the other hand, the thermal model covers all the correlations and equations needed to describe the heat transfer between the fluid and the atmosphere. The solving of the numerical equations is based on discretizing equation (14) and assuming that the average fluid temperature in the storage tank (T_{st}) is equal to the inlet temperature of the receiver (T_{in}). At the initial stage, T_{in} is estimated to be equal to the ambient temperature. Then, equations (8) and (9) will be used to evaluate the instantaneous thermal power and outlet fluid temperature respectively. This sequence of calculation will be repeated by incrementing the time by Δt until the time increment is equal to the sunset time when the PTC returns to the initial position. Finally, it is worth mentioning that the calculation of T_{in} at the instant $t+\Delta t$ is based on the calculated value of the outlet temperature of the receiver T_{out} at the instant t.

5 Results and discussions

In order to investigate the effect of different sun tracking configurations on the thermal performance of the PTC, the thermal production has been chosen as a meaningful indicator instead of the instantaneous thermal efficiency, due to the former's cumulative aspect over the year. Hence, the thermal energy will be evaluated every ten minutes from January 1 to December 31 (2016). Several scenarios will be considered according to the sun tracking or fixed configuration. The surface azimuth angle is set at 0° (except for the two-axes sun tracking configuration).

5.1 Fixed installation

5.1.1 First scenario, the collector tilt angle w = 15°

When the PTC's tilt angle (angle between the horizontal plane and the aperture area) is fixed at 15°, the thermal production of the installation is much higher in summer period, between April and September (days from 91 to 244), as depicted in Figure 2. Indeed, in this period the installation delivers an average of 12 kWh per day instead of 9.6 kWh per day in the rest of the year. This is mainly justified by the fact that the apparent sun path in the sky during this period is higher, which allows to the aperture of PTC to stay mostly in front of the sun and hence to collect

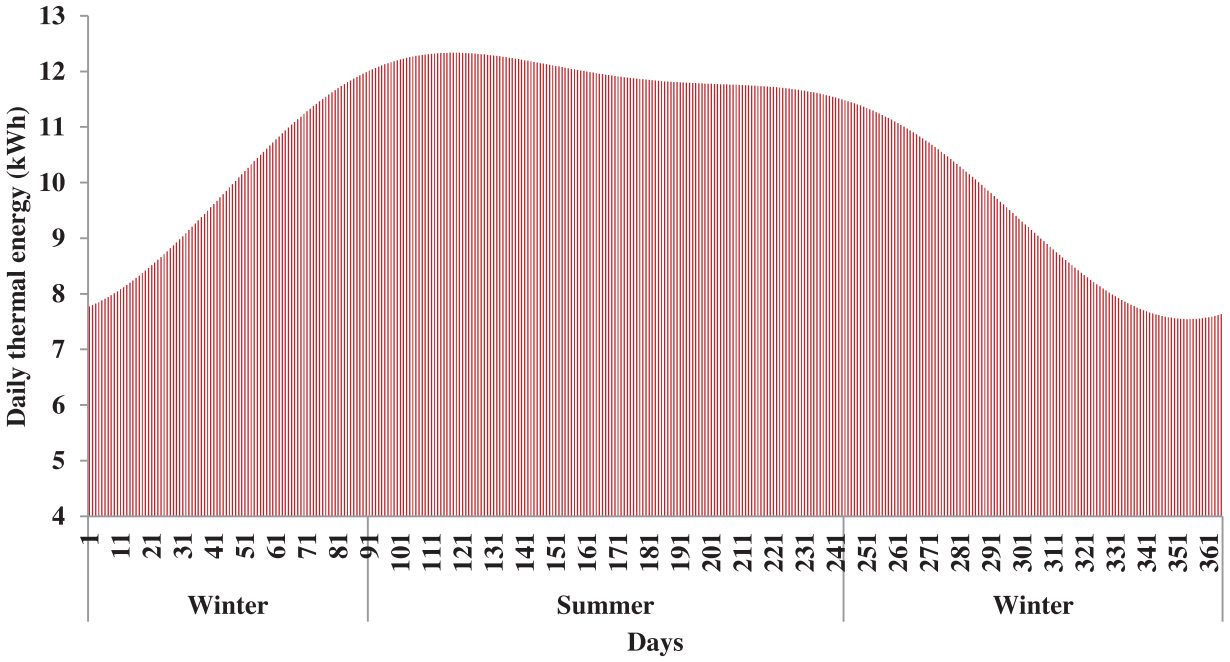

Fig. 2. Variation of daily thermal energy throughout the whole year (2016), tilt angle w = 15°.

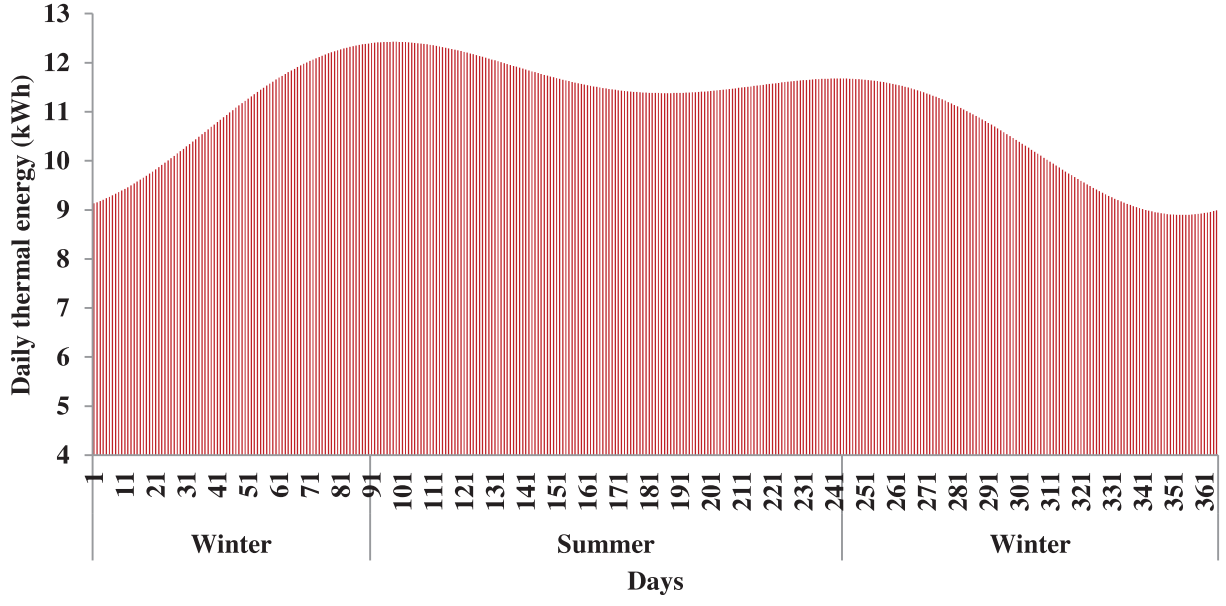

Fig. 3. Variation of daily thermal energy throughout the whole year, tilt angle w = 25°.

maximal direct solar irradiance. Contrary to the rest of the year (winter) when less direct solar irradiance is collected, as a result of the lower apparent sun's elevation.

5.1.2 Second scenario, w = 25°

In this scenario (see Fig. 3), the thermal energy produced by the installation has been slightly improved by 10.6% during the winter compared to the first scenario. Indeed, the daily average of the total production in this period has been increased from 9.6 to 10.6 kWh. However, in summer period, the daily average of thermal energy has been slightly decreased to 11.76 kWh. But, from an annual perspective, the annual thermal energy was improved by 4.5%.

5.1.3 Third scenario, w = 35°

This scenario corresponds to the latitude of the studied region; it provides a balanced thermal gain throughout the year with a significant improvement in thermal

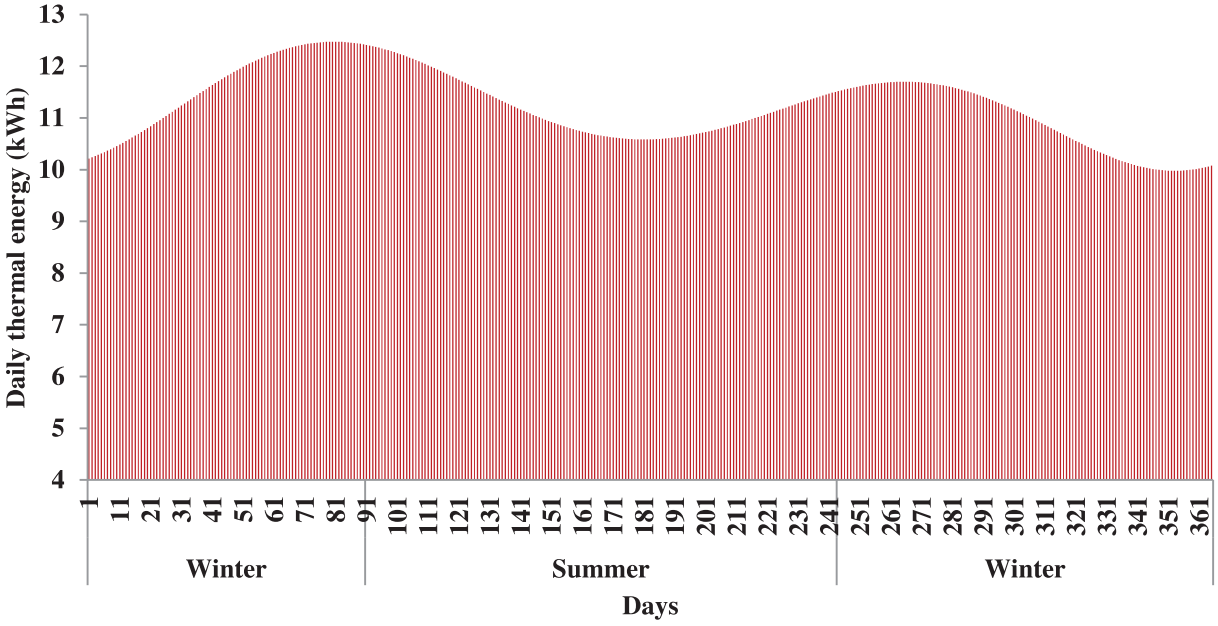

Fig. 4. Variation of daily thermal energy throughout the whole year, tilt angle w = 35°.

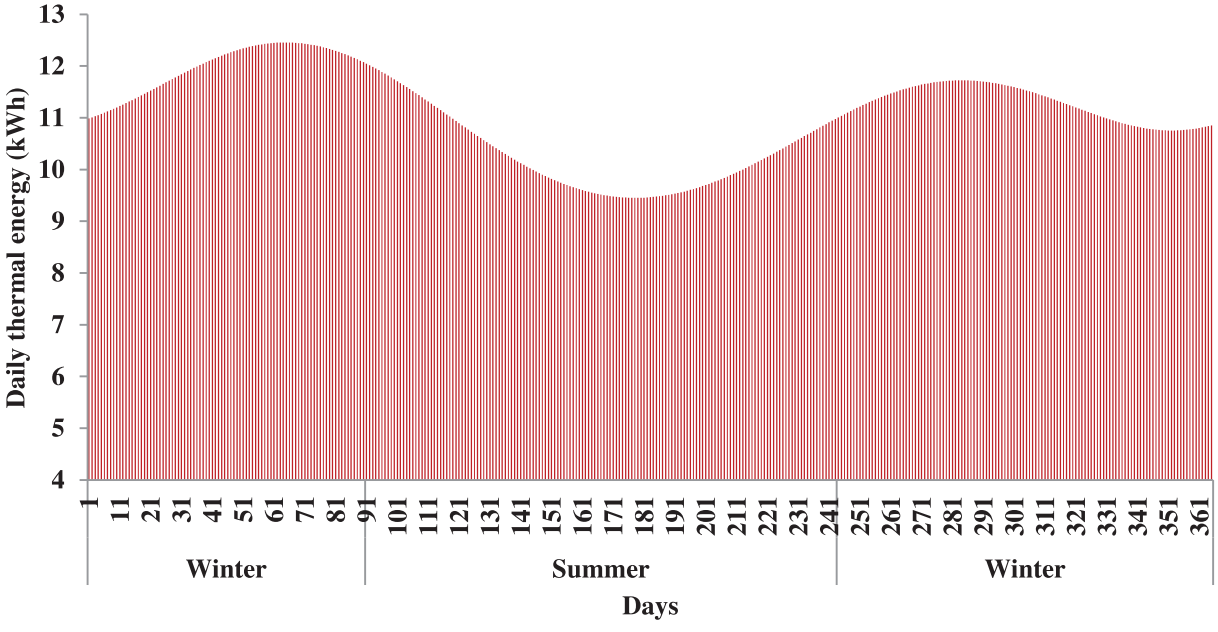

Fig. 5. Variation of daily thermal energy throughout the whole year, tilt angle w = 45°.

performance of the installation during the winter, as shown in Figure 4. In fact, the PTC generates a daily average of 11.27 and 11.20 kWh during the winter and summer periods respectively. Similarly, the annual thermal energy has been improved by 5.9%. These results are in line with several publications in the literature that confirmed that the optimal slope angle of solar systems corresponds to the latitude of the site.

5.1.4 Fourth scenario, w = 45°

Given the fact that the sun's elevation angles vary mostly between 40 and 77° in summer period, the aperture area of the PTC in this scenario does not receive considerable amounts of direct sun radiations, which affects significantly the thermal energy delivered in this period (see Fig. 5); indeed, the average thermal energy produced per day decreases by 14% compared with the first scenario, to reach 10.30 kWh. This decline impacts also the annual thermal energy which decreases by 1.5% compared to the third scenario. However, it is worthwhile to notice that this scenario recovers a great amount of direct sun rays during the winter and enhance the daily thermal energy produced in this period to attain 11.62 kWh.

To sum up, the results of the four scenarios have been illustrated in Table 2. Accordingly, it is worth noting that the suitable choice of the tilt angle for the adequate

Table 2. Summary of the thermal energy produced in function of tilt angle and seasons.

Tilt angle (°)	15	25	35	45
Summer (kWh)	2165.53	2147.39	2064.07	1918.10
Winter (kWh)	1685.03	1885.77	2029.29	2111.21
Annual (kWh)	3850.55	4033.16	4093.35	4029.31

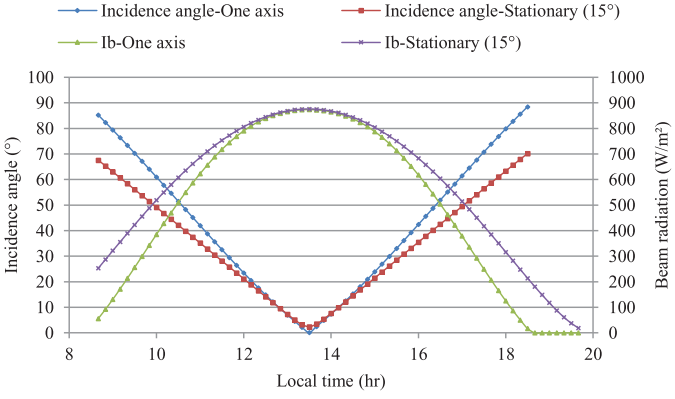

Fig. 6. Variation of incidence angle and beam radiation on July 21 for both stationary and one-axis tracking configurations.

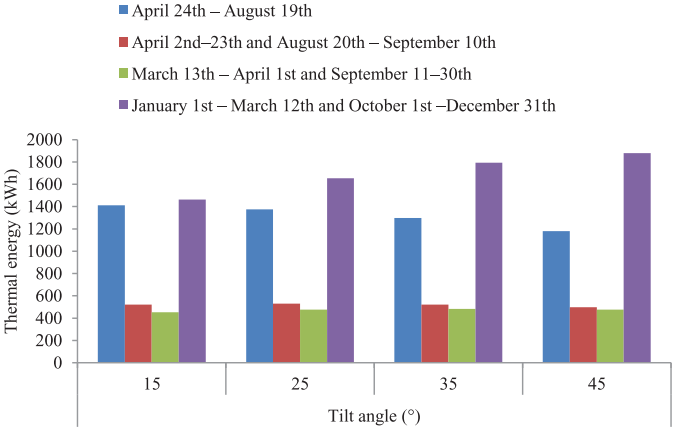

Fig. 7. Distribution of thermal energy versus the tilt angle throughout the year.

application could be a highly sensitive issue, since it impacts significantly the thermal performance of the installation. Moreover, the optimum tilt angle varies from one season to another. Thus, in our case study, even if 35° could be considered as the optimal tilt angle during the whole year, other scenarios could be more efficient in some specific periods. Consequently, a seasonal monitoring is required to maximize the thermal production throughout the year.

5.2 Semi-automatic installation

In this section, a new sun tracking configuration will be investigated to overcome the probable declines of the thermal performance dictated by the seasonal suitability of the fixed tilt angles. In fact, the stationary configuration could be more efficient than the one-axis sun tracking configuration in some specific periods of the year; for instance, in summer period, the incidence angle is mostly lower for an installation with a 15° inclination than a one-axis sun tracking configuration, as shown in Figure 6, that exhibits the daily variation of the incidence angle and the beam radiation on July 21. From this figure, it is obvious that the stationary installation is in a better position to receive more direct sun radiation, hence to produce more thermal energy, which is the reason behind the proposition of the new sun tracking configuration that consists of varying periodically the PTC's tilt angle according to the produced thermal energy. For example, for a tilt angle of 15°, the thermal performances reach their maximum between May 24th and August 19th (days from 144 to 231), and so on.

The periodical distribution of the tilt angles during the year according to the thermal performances as well as their respective thermal production have been schematized in Figure 7 that depicts the variation of the annual thermal energy produced by the PTC according to the proposed new sun-tracking configuration. The new installation's production profile combines between the maximum thermal performances of the four configurations studied above. The results have revealed an improvement of 4.9% when compared with the optimum configuration of the stationary installation (w = 35°).

5.3 Automatic installation

5.3.1 One axis sun tracking

In this section, the PTC's tilt angle will be varied continuously every ten minutes according to the sun's apparent position. The findings have been schematized in Figure 8 that represents the variation of the annual thermal energy for different sun tracking configurations. From this figure, one can notice that this tracking approach has improved the thermal performance in winter period. Accordingly, the annual thermal production has been enhanced by 1.24% compared to the optimal configuration. However, it remains less efficient than the new proposed tracking mode by 3.65%.

5.3.2 Two-axes sun tracking

This configuration is based on the same principle of one axis sun tracking system; the only difference is that the PTC's azimuth angle is varied as well.

From Figure 8, it can be concluded that, in terms of thermal performance (regardless of the electrical energy

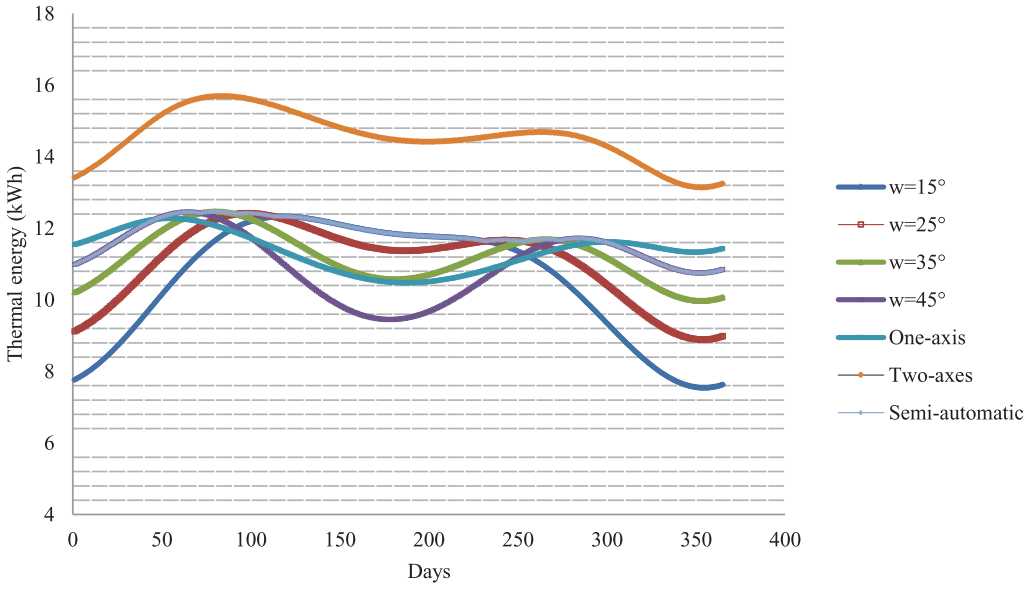

Fig. 8. Variation of the daily thermal energy production according to sun tracking or fixed configuration.

consumption), the two-axis sun tracking is the best configuration; in fact, it allows improving the thermal production by 23%, 22% and 19% compared to the optimal configuration of fixed installation, one-axis and semi-automatic configurations, respectively. This is justified by the fact that the tilt and the azimuth angles are varied instantaneously, thus the angle of incidence is reduced. Therefore, the PTC receives maximum direct sun rays.

Finally, based on the finding of the numerical simulations of different sun tracking approaches, it is worth highlighting the fact that semi-automatic sun-tracking configuration is a promising alternative to reduce the electrical consumption of the tracking device and enhance the thermal performance of the installation, since it exceeded the thermal production of the one-axis tracking configuration. Hence the emergence of a new efficient sun tracking approach that could be justified through an economic study in a future work. However, the two axes sun tracking method remains by far the best configuration to have better thermal performance all over the year.

6 Model validation

The mathematical model used for simulating the impact of different sun tracking configurations on the performance of a PTC was verified and validated by comparing the hourly thermal power calculated in the current work with the experimental findings of two other publications. The first one [22] exhibits the variation of the beam radiation on an inclined surface based on the measured beam radiation on a horizontal surface generated by the METEONORM database. The reported values, under climatic conditions of Ouarzazate city (Morocco), have been substituted into equation (8) to calculate the generated thermal power on

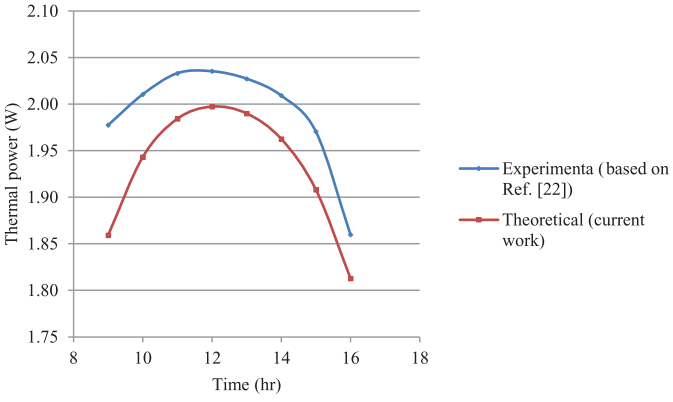

Fig. 9. Hourly variation of thermal power on July 7.

July 07. The results have been plotted in Figure 9 along with the hourly variation of the thermal power calculated by the mathematical model. The comparison has shown a very good agreement between the results of the current work and that proposed by [22]; indeed, the average relative error between the results of the mathematical model and those based on experimental values is remarkably low (2.93%) which confirms the accuracy of the mathematical model.

Similarly, the second validation was fulfilled by comparing the calculated thermal power using experimental values of the beam radiations in Biskra city (Algeria) reported by [23]. The thermal profile displayed by the current mathematical model has the same variation path as the experimental one with a slight difference in the slope coefficient as shown in Figure 10; indeed, the main relative error is 3.96% which corresponds to thermal power's variation on June 21.

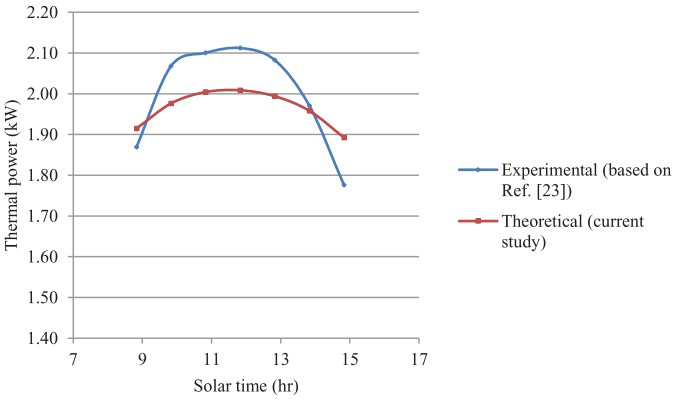

Fig. 10. Hourly variation of thermal power on June 21.

7 Conclusion

The objective of this work was to develop the thermal profile of a thermal solar system with a parabolic trough collector in Tangier and to study the impact of the sun tracking methods on its thermal performances. Indeed, several numerical simulations have been carried out for different configurations of sun tracking: fixed installation, semi-automatic installation and full automatic installation. The results of the current mathematical model have been compared with some experimental findings available in the literature; this comparison has confirmed the validity of the theoretical model with a significantly low relative error (2.93%).

Based on the numerical investigation results, the main findings are summarized as follows:

– Fixed installations, which are not equipped with a sun tracker, have better thermal production at certain times of the year.
– In Tangier city, 35° is the optimum tilt angle which has a balanced production all over the year.
– The semi-automatic system performs better than one-axis sun tracking system. Indeed, a periodic change of the tilt angles during the year improves the thermal production of the studied installation by 4.9% compared with the optimum stationary configuration and it is more efficient than one axis sun tracking configuration by 3.65%. Furthermore, the electrical energy consumption of the semi-automatic sun tracking device is obviously less important than that of the continuous trackers.

Nomenclature

A	Area (m^2)
B	Atmospheric extinction coefficient (–)
C_p	Specific heat (J/kg. °C)
C_{pmet}	Specific heat of the storage tank (J/kg. °C)
D	Diameter (m)
F^{-}	Efficiency factor of collector (–)
F_r	Heat removal factor of collector (–)
H_{alt}	Altitude above sea level (m)
H_{ab}	Absorbed solar irradiance (W/m^2)
$h_{\mathrm{r-ra}}$	Radiation heat transfer coefficient between receiver and surrounding environment ($W/m^2.°C$)
$h_{\mathrm{c,i}}$	Convective heat transfer coefficient between receiver and fluid ($W/m^2.°C$).
h_w	Convective heat transfer coefficient between receiver and surrounding environment ($W/m^2.°C$)
I_b	Beam solar irradiance (W/m^2)
I_{bn}	Direct normal irradiance (W/m^2)
K_r	Conductivity of receiver (W/m. °C)
m_f	Mass flow rate (kg/s)
M	Mass (kg)
ND	Number of the day in the year
P_L/P_0	Ratio between the pressure of the geographical site and atmospheric pressure (–)
$Q_{u,\mathrm{th}}$	Useful thermal power (W)
T	Temperature (°C)
T_{st}	Average fluid temperature in the storage tank (°C)
U_l	Overall heat loss coefficient ($W/m^2.°C$)
w	Collector tilt angle (°)

Subscripts

ap	Aperture area
ab	Absorbed
alt	Altitude
amb	Ambient
b	Beam
bn	Direct normal
ext	External
f	Fluid (water)
in	Inlet
int	Internal
met	Metal (storage tank)
out	Outlet
r	Receiver
st	Stored water

Greek symbols

θ_e	Sun altitude angle (°)
θ_z	Sun zenith angle (°)
θ	Incidence angle (°)
γ	Collector azimuth angle (°)
Γ	Sun azimuth angle (°)
η_{th}	Thermal efficiency
ρ	Reflectivity of the reflector (–)
α	Absorptance (–)

Abbreviations

CPC	Compound Parabolic Collector
CSP	Concentrated Solar Power
PTC	Parabolic Trough Collector

References

1. A. El Fadar, Energy **114**, 10 (2016)
2. H. Mousazadeh et al., Renew. Sustain. Energy Rev. **13**, 1800 (2009)
3. M.J. Clifford, D. Eastwood, Sol. Energy **77**, 269 (2004)
4. W. Nsengiyumva, S.G. Chen, L. Hu, X. Chen, Renew. Sustain. Energy Rev. **81**, 250 (2018)
5. K.K. Chong, C.W. Chong, Sol. Energy **13**, 298 (2009)
6. N.A. Kelly, T.L. Gibson, Sol. Energy **83**, 2092 (2009)
7. F.R. Rubio, M.G. Ortega, F. Gordillo, M. López-Martínez, Energy Convers. Manage. **48**, 2174 (2007)
8. T. Maatallah, S.E. Alimi, S.B. Nassrallah, Renew. Sustain. Energy Rev. **15**, 4053 (2011)
9. A. Khalifa, S.S. Al-Mutawalli, Energy Convers. Manage. **39**, 1073 (1998)
10. B. Barakat, H. Rahab, B. Mohmedi, N. Naiit, in *Proceedings of the Fourth Jordanian International Mechanical Engineering Conference JIMEC 2001*, 471–488
11. S. Abdallah, S. Nijmeh, Energy Convers. Manage. **45**, 1931 (2004)
12. J. Sun, R. Wang, H. Hong, Q. Liu, Appl. Therm. Eng. **112**, 1408 (2017)
13. A. Salsabila, S. Suhaidi, Z.A. Mohd, Procedia Environ. Sci. **17**, 494 (2013)
14. Y. Wang, Y. Zhu, H. Chen, X. Zhang, L. Yang, C. Liao, Appl. Therm. Eng. **87**, 381 (2015)
15. W. Qua, R. Wanga, H. Honga, J. Suna, H. Jina, Energy Procedia **105**, 780 (2017)
16. J. Meeus, in *Astronomical algorithms* (Willmann-BELL, Inc., 1998), p. 59
17. I. Reda, A. Andreas, Solar Position Algorithm for Solar Radiation Applications (National Renewable Energy Laboratory, 2008), NREL/TP-560-34302
18. A.Y. Tadahmun, Anbar J. Eng. Sci. **5**, 109 (2012)
19. M. Esmail, A. Mokheimer, Energy Convers. Manage. **86**, 622 (2014)
20. A. Fahad, Energy **58**, 561 (2013)
21. A. El Fadar, A. Mimet, M. Pérez-García, Sol. Energy **83**, 850 (2009)
22. A. Allouhi, M. Benzakour Amine, T. Kousksou, A. Jamil, K. Lahrech, Appl. Therm. Eng. **128**, 1404 (2018)
23. A. Moummi, N. Hamani, N. Moummi, Z. Mokhtari, Estimation du rayonnement solaire par deux approches semi empiriques dans le site de Biskra, in *8th International Meeting on Energetical Physics*, https://www.researchgate.net/publication/264781835

Cite this article as: O. Achkari, A. El Fadar, Thermal performance comparison of different sun tracking configurations, Eur. Phys. J. Appl. Phys. **88**, 20902 (2019)